Performance Comparison of the Standard Photovoltaic Thermal Collector (PVT) and Photovoltaic Thermal Collector with Phase Change Materials (PVT-PCM)

Muhammad Syazwan Aziz*⬤, Adnan Ibrahim*‡⬤, Muhammad Amir Aziat Bin Ishak*⬤, Anwer. B. Al-Aasam *⬤, Ahmad Fazlizan*⬤, Ag Sufiyan Abd Hamid**⬤,

* Solar Energy Research Institute, Universiti Kebangsaan Malaysia, Bangi, Selangor, 43600, Malaysia

** Faculty of Science and Natural Resources, Universiti Malaysia Sabah, Kota Kinabalu 88400, Malaysia

(azizmsyazwan@gmail.com, iadnan@ukm.edu.my, amiraziat93@gmail.com, anwor.bassim@gmail.com, a.fazlizan@ukm.edu.my, pian@ums.edu.my)

‡Adnan Ibrahim, Solar Energy Research Institute, Universiti Kebangsaan Malaysia, 43600, Bangi, Selangor, Malaysia, Tel: + 60 389118581, iadnan@ukm.edu.my

Abstract- The purpose of this study is to evaluate the thermal and electrical efficiency of PVT-PCM and PVT for photovoltaic thermal collectors. A square absorber tube with PCM was utilized in the study, introducing a new approach to photovoltaic thermal collectors. COMSOL computational fluid dynamics (CFD) software was employed to carry out the simulations, and the tests were conducted as indoor experiments in a lab. Water was used as the transmission fluid in this study. Different volume flow rates ranging from 1–3 LPM were assessed for both experiment and simulation by considering the radiation range of 400, 600, and 800W/m². At a volume flow rate of 2 LPM, experimental results showed that PVT-PCM achieved higher electrical and thermal efficiencies of 9.95% and 88.3%, respectively, compared to the simulation results of 10.0% and 86.5%. Comparable outcomes were seen with both the simulation and experiment.

Keywords Jet impingement, Photovoltaic Thermal (PVT), Heat transfer, Solar collector, CFD simulation

1. Introduction

The overall efficiency of photovoltaic systems has increased with continuous expansion in solar energy applications. Conventional photovoltaic (PV panels) differs based on the composition material, but in order to produce electricity, the PV panels generally only need photon from light [1]–[3]. However, solar radiation's heat causes the temperature of PV panels to inflate, which reduces their electrical efficiency [4]. Cooling methods can be introduced to avoid this reduction [5], [6]. One method would be combining the collectors into a hybrid system called Photovoltaic-Thermal (PVT). Most current PVT research studies have concentrated on systems that employ water as a heat transfer fluid because of the higher heat capacity when contrasted with air, enabling the system to continue year-round operation [7]. Due to this, better efficiencies of thermal and electrical can be achieved with water systems versus air systems. Other benefits include space conservation and

reduced installation costs when the two systems are integrated into one place [8]–[10]. Furthermore, it can be said that PVT systems could be further enhanced by employing alternative design structures and materials in an appropriate quantity without resulting in bad energy prices or prolonged payback periods [11]–[14]. PVT units' combined thermal and electrical efficiencies were identical to the overall efficiency because PVT systems are segmented on the employed working fluid as well as the configurations of the collector. Another option would include the collector being a tube, heat pipe, sheet, or others [15], [16]. To enhance the overall system efficiency, various collector configurations have been examined for different systems [17], [18].

A water-based photovoltaic thermal simulation employed seven new absorber collector design configurations. A range of rectangular and round hollow tubes was considered to choose the cross-sectional shape of the absorber. The most efficient one was the spiral flow design, which had a cell

efficiency of 11.98% and a thermal efficiency of 50.12% [19]. Ibrahim et al. built a pair of PVT water collectors. One collector would be a spiral flow absorber, and the other would be a single-pass rectangular tunnel [20]. According to the data, the spiral flow configuration achieved the maximum electrical and thermal efficiency levels. Three PVT water collectors were developed and compared by Sopian et al. regarding thermal performance before fabricating prototypes [21]. The first was a direct collector, the second was a parallel collector, and the third was a split flow collector. PVT systems with split flow designs are deemed more efficient since cold water passes from both sides of each flow. Thus, a split-flow design can increase a water-based PVT system's thermal and electrical efficiency. Mihai et al. [22] propose an innovative technical solution for increasing PVT efficiency by equipping PV panels with a cooling system and integrating a water-to-water heat pump with hot water storage, resulting in an overall increase in efficiency of up to 45%, and making it more competitive than separate use of PV panels and solar collectors. Barbu et al. [23] investigated the potential solution of integrating solar renewable energy in the district heating by using a system of PVT to cover the domestic hot water (DHW) requirements of the end-users, which generated both electricity and heat in a micro-cogeneration system with good thermal and energy outputs.

The main functions of PCMs in PVT include improved cooling for PV modules and thermal energy for working fluid flow via thermal collectors [24], [25]. Moreover, the heat of a PV module can be controlled using PCM materials, which can hold a considerable amount of heat when they transition from solid to liquid. Although such materials could be liquid or solid, they absorb sensible heat. This phenomenon helps to eliminate heat from objects like solar panels when in close contact.

The performance pertaining to a PVT system in the presence and absence of PCM was numerically compared by Gaur et al. in France [26]. The temperatures of different system components were evaluated by designing a thermal model. During winter, achievement of 16.5% and 16.87% of electrical efficiency was possible, while a specific range of ambient temperature and solar irradiation was employed in this study. As per Fayaz et al., the heat transfer and performance of water-based PVT systems can be improved with PCM [27]. Kyaligonza et al. [28] utilized a 3D numerical model to compare four solar module configurations and validate their proposed three configurations of PVT-PCM, which achieved the highest conversion efficiency and specific electrical power per unit area and found that a 0.5m/s increase in inlet velocity resulted in a 0.06% increase in efficiency.

Hussein et al. [29] conducted experiments and numerical simulations to evaluate the electrical and thermal performance of three types of PVT flow configurations: direct, web, and spiral flow. The results show that PVT systems have higher efficiency in converting solar radiation energy to electrical and thermal energy than conventional PV modules. The spiral flow collector achieved the highest electrical efficiency of 9.1%, while the spiral flow and direct flow collectors had the highest overall efficiencies of 35% and 27.5%, respectively. The PVT web flow system exhibited the highest temperature

of 68C for the PV module, while the spiral flow system achieved the lowest temperature of 45.2C. Al-Waeli et al. [30] used a nanofluid and nano-PCM-based PVT to improve a PV module's electrical performance and characteristics, obtaining a maximum PV efficiency of 13.7% compared to 7.1% for a conventional PV module.

This paper presents a novel approach to enhancing the thermal performance of the PVT system by using a square absorber tube with PCM. The study analyzed the impacts of PCMs and thermal collectors separately for PVT systems. The numerical performance of the systems was evaluated and compared to different thermal collector designs. Additionally, the effects of solar radiation level and mass flow rates on temperature and overall system performance were assessed for the system.

2. Research Description

Three different water flow rates (1, 2, and 2.5 L/min) and three different radiation levels (400, 600, and 800W/m^2) were used to evaluate the system numerically and experimentally. These systems were connected to solar panels, one without PCM signifying PVT while the other employing PCM signifying PVT-PCM. The models were validated via experiments. The systems have been designed based on comparable-sized elements and generally use the same designs and calculations as the numerical models. The spiral-designed absorber tube is attached to the PV panel by eliminating any air gap between them to enhance heat transmission.

2.1. Numerical Investigations

The 3D models have been created by using COMSOL software. Therefore, a square cross-section is present for the absorber tubes of these models. Fig. 1 depicts the PVT and PVT-PCM systems.
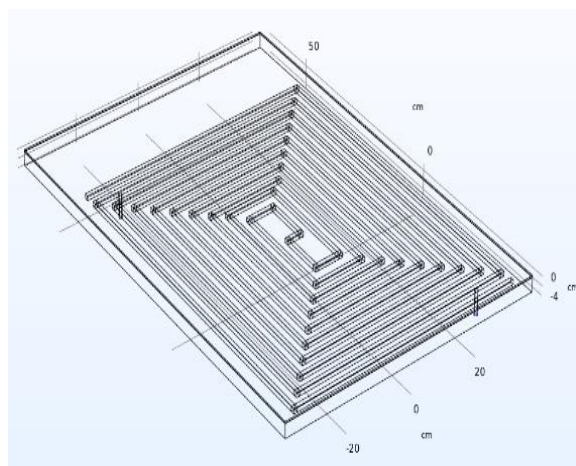
Fig. 1 PVT and PVT-PCM systems

Table 1 Properties of solar module's layers [31]

Layer	Thickness (m)	Density (kg/m3)	Thermal conductivity (W/m.K)	Specific heat capacity (J/kg.K)

Tempered glass	0.032	2450	0.7	790
EVA	0.0005	960	0.311	2090
PV cell	0.00021	2330	130	677
PVF	0.0003	1200	0.15	1250

Table 2 Properties of Paraffin Wax [32]

Properties	Solid phase	Liquid phase
Melting point	56 (ºC)	56 (ºC)
Latent heat	142.7 (kJ/kg)	142.7 (kJ/kg)
Thermal conductivity	0.4 (W/m ºC)	0.2 (W/m.ºC)
Density	670 (kg/m^3)	640 (kg/m^3)
Specific heat	2.4 (kJ/kg ºC)	1.6 (kJ/kg ºC)

The COMSOL software ran a 3D numerical simulation in stationary state conditions. The simulation assumes the following: 100% transmissivity to be present in the EVA PV layer, no dust on the PV surface can impact solar energy absorption, and the flow is incompressible and laminar. The following can be regarded to be the key partial differential equations as thermal energy equations for fluid and solid layers and continuity and momentum equations pertaining to fluid layers:

Thermal energy equation [33], [34]:

$$\rho C_P u. \nabla T + \nabla. q = Q + Q_{ted}, q = -k\nabla T \quad (1)$$

Continuity equation:

$$\rho \nabla. u = 0 \quad (2)$$

Momentum equation:

$$\rho(u.\nabla)u = \nabla.[-Pl + K] + F \quad (3)$$

Regarding the fluid, structural and explicit simulations, COMSOL meshing technologies provide physics choices that aid in automating the meshing process. The program will adjust to more logical meshing settings if the physics option is set in the software. Boundary conditions are based on the following [35]–[38]:

1. At the top surface of the PVT: General inward heat flux

2. At the top surface of the PVT: diffuse surface condition

$$-n. q = \varepsilon\sigma(T_{amb}^4 - T^4), \quad (4)$$

where σ is the Stefan-Boltzmann constant

3. At the top surface of the PVT: convective heat flux

$$q_o = h.(T_{ext} - T) \quad (5)$$

4. At the side boundaries of the PVT module: insulation

$$-n. q = 0 \quad (6)$$

5. At all solid boundaries of the fluid passing path: no-slip condition

$$u = v = w = 0 \quad (7)$$

6. At the inlet:

mass flow rate $m = mdot$, and $T = T_{in}$ \quad (8)

7. At the outlet:

$$p = 0 \quad (9)$$

Laboratory-based experimental data were used to verify the present 3D simulation of the PVT. Comparing the simulation's heat efficiency findings versus the experimental results and the results from Adnan et al.'s system [26]. Furthermore, these numerical results aligned with photovoltaic thermal collectors (PVT) performance with different absorbers designs [19]. As shown in Table 3, this simulation could offer reliable results to analyze and validate the PV performance.

Table 3 Simulation results validated with experimental.

Adnan et al. [19]		Present simulation work		Present experimental work	
GT	η$_{th}$	GT	η$_{th}$	GT	η$_{th}$
437.13	51.84	400	45.04	400	43.39
631.40	52.15	600	53.78	600	50.25
812.72	52.13	800	58.11	800	58.64

In a real-world scenario, wind speed and solar radiation keep changing constantly. The PVT system is regarded to be dynamic with regard to functioning. Due to this, the 3D stationary model can be deemed a viable alternative to deal with challenges and ambiguities pertaining to time-consuming 3D dynamic models. Thus, the current examination employs 1000 W/m^2 of radiation for the experiment.

2.2. The experimental Investigations

The systems have been evaluated in an experimental indoor setup; Fig 2 and 3 demonstrate the system and the equipment employed in the experiment. Indoor tests in the laboratory can yield accurate measurements since, in such situations, solar radiation can be controlled. This study employed three PV modules. A conventional PV module was the first one. The second PV panel was linked to the spiral design of a tube absorber as a PVT system, and the final one has deemed the same PVT system as PCM. The specification was identical since testing of all models was done on the same PV panel.

Fig. 2 PVT / PVT-PCM back-end system

This segment discusses the components and tools used to gather data in this experiment. An AC-power-supply transformer-powered solar simulator with 70 500-W halogen lights was deployed for supplying irradiance to solar systems. Standard equipment and gear were used to gather data from the research. The TES 132 solar power meter, a digital flow meter DHYB-800, a thermocouple k-type, an IV tracer PROVA 1011, and a data taker DT 85 were a few of the most crucial tools and technologies used. Instruments were affixed to the systems at the necessary places to gather data, which was then scrutinized to accomplish the study's objectives. The instruments do not function perfectly, and each comprises some error. Table 4 shows the error rate of the instruments utilized in the tests. Table 5 shows that the used model of the PV panel was VE-100-36M model specifications.

Fig. 2 PVT / PVT-PCM back-end system

Table 4 The experiment's measuring equipment.

Instruments	Error rate
TES 132 solar power meter	$\mp 10 \ W/m^2$ or 5%
thermocouple k-type	0.1 ºC
A digital flow meter DHYB-800	0.5%

Table 5 The specifications of the PV panel

Electrical performance under Standard Test Conditions (STC)	
Rated Maximum Power Pmax	100 W
The voltage at Maximum Power Vmp	18.59 V
Current at Maximum Power Imp	5.38 A
Open Circuit Voltage Voc	22.42
Short Circuit Current Isc	5.76 A

Water flow is initiated to regulate and stabilize the requisite flow precisely. The tests were conducted such that the parameters' accuracy was well preserved. Next, the solar simulator was activated per the volumetric flow rate to prevent any pre-heating of the components from obtaining accurate outcomes. It was observed that the data remained stable with practically no change after 20-30 minutes, subject to various volumetric flow rates.

Each sample's data were compared and analyzed for any substantial inaccuracies or differences. Nonetheless, the researchers considered the data produced after at least an hour of testing to ensure stability and to prevent any errors or ambiguities in the data. The schematic arrangement of the internal experimentation, including all equipment and parts, their location, and fixtures, is systematically illustrated in Fig. 4.
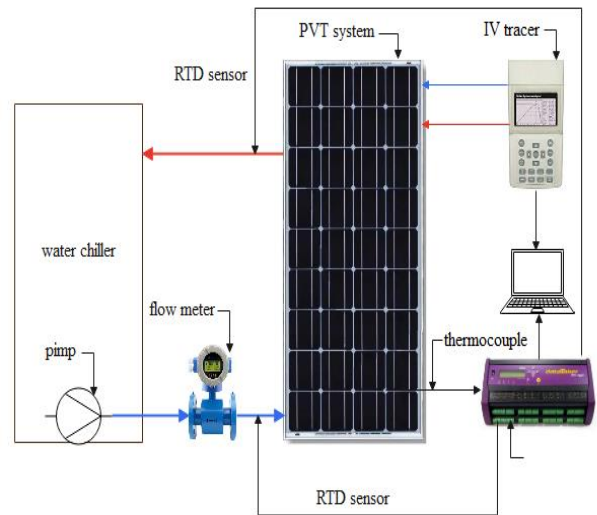
Fig. 4 Schematic diagram of an indoor experimental setup including all components and equipment.

Most instruments have inaccuracies, where inaccuracy is defined as the difference between what it does and reads. Some instruments are complex to calibrate, while some can be easily calibrated, and errors can be reduced to obtain accurate readings. Nonetheless, in most cases, errors cannot be overlooked entirely. Thus, uncertainty evaluation is required to understand equipment-related errors that may develop in the investigation. For the evaluation of uncertainty, Eq. (1) has been used [39]

$$W_R = \left[\left(\frac{\partial R}{\partial \chi_1} \omega_1 \right)^2 + \left(\frac{\partial R}{\partial \chi_2} \omega_2 \right)^2 + \cdots + \left(\frac{\partial R}{\partial \chi_n} \omega_n \right)^2 \right]^{0.5} \quad (10)$$

W_R represents uncertain outcomes. $(\omega_1, \omega_2, \ldots, \omega_n)$ are the independent variable uncertainties, whereas R is a known function of $(\chi_1, \chi_2, \ldots, \chi_n)$. Before extrapolating to additional experiments, the uncertainty in the present research's statistics was estimated as in Table 6. The result has an uncertainty of less than 3%, which is a good indication of the precision of the measurement.

Table 6 The PVT system measurements' uncertainties.

The uncertainty	Symbol	Value
In the thermal efficiency	W_{R1}	1.96%
In the electrical efficiency	W_{R2}	1.00%
In the experiment's overall	W_R	2.20%

3. Evaluation Results and Rationale

3.1. Effects of mass flow rate on thermal efficiency

Thermal efficacy is dependent on temperature differential and mass flow rate. Figs. 5, 6, and 7 illustrate the differences in water outlet temperature and thermal efficacy from Eq. (11) with the values of the volume flow rate 1, 1.5, and 2 LPM under solar irradiation of 400, 600, and 800 W/m² [40], [41].

$$\eta_{th} = m^o C_p (T_o - T_i)/I * A \qquad (11)$$

Where m^o represents mass flow rate, C_p represents the specific heat capacity of heat transfer fluid, T_o represents outlet temperature, T_i represents inlet temperature, I is the solar irradiance intensity, and A represents the collector area.
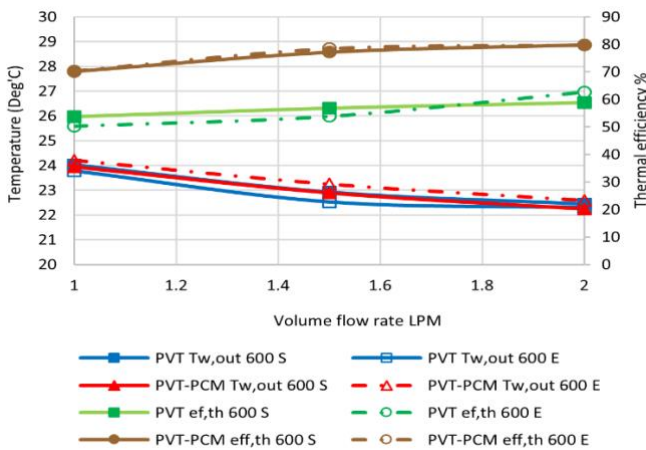
Fig. 5 Changes in water outlet temperature and thermal efficiency with various volume flow rates under 400 W/m² solar irradiance
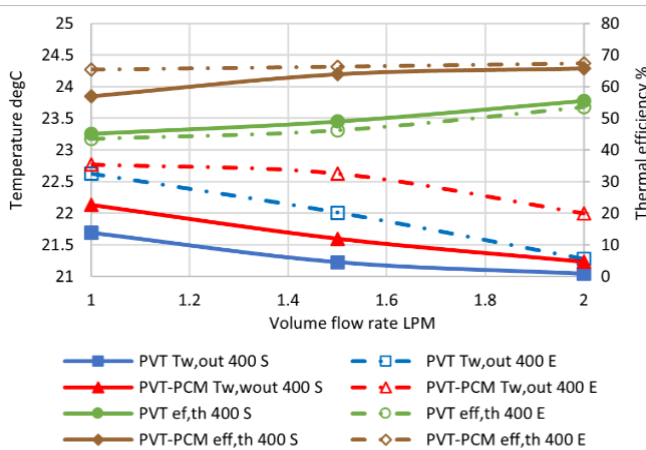
Fig. 6 Changes in water outlet temperature and thermal efficiency with various volume flow rates under 600 W/m² solar irradiance
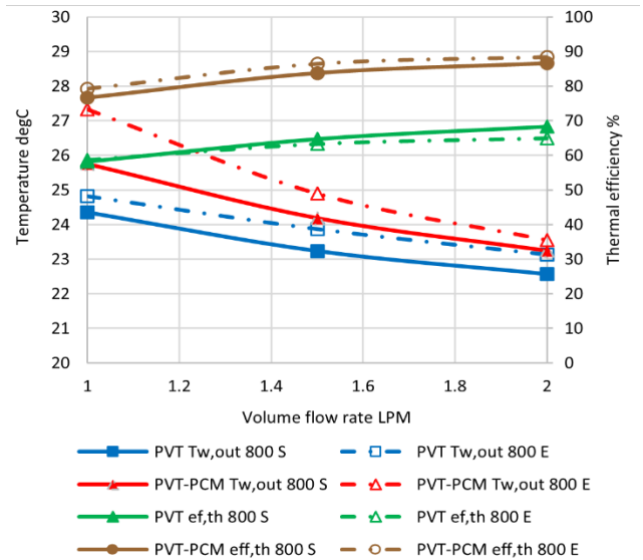
Fig. 7 Changes in water outlet temperature and thermal efficiency with various volume flow rates under 800 W/m² solar irradiance

Adding PCM to the PVT system significantly improved since the thermal efficacy rose by about 15% in all situations. Nonetheless, there was no entire match between the theoretical estimates and experimental outcomes since ideal conditions were used in the simulation, while the experimental conditions were practically the same. The experiment was conducted under laboratory conditions, with cooling equipment regulating the inlet temperature of the water ranging from 19 to 22 degrees. For simulation, water was assumed to be at 20 degrees, and the PV surface was exposed to radiation values of 400, 600, and 800W/m². Additionally, solar simulators were employed, and there was a very small deviation of ∓50 W/m² between the required radiation intensity and the PV surface area's radiation intensity. Fig. 8 illustrates the PV panel surface temperature distribution with the solar radiation change for both systems, PVT-PCM and PVT. Even though PCM use significantly decreases the temperature in regions not having tubes for cooling under the PV, the highest PV surface temperature is displayed in Figs. 9 and 10.
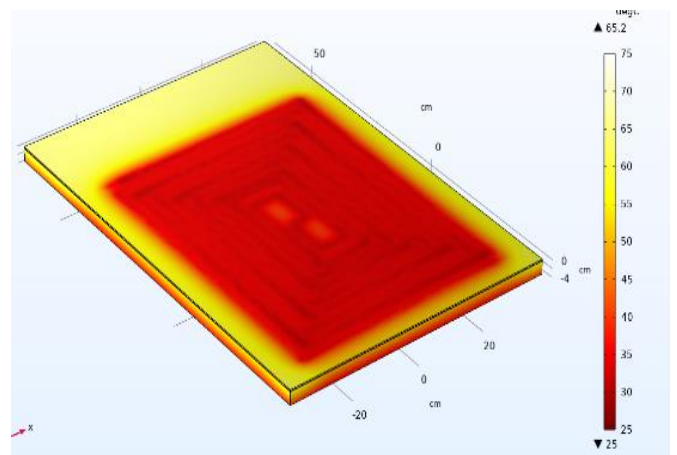
Fig. 8 Temperature distribution of the system at volume flow rate 2 LPM and 600 W/m² PVT-PCM

Although using Phase Change Material (PCM) can significantly reduce the temperature in regions without cooling tubes under the PV module, the highest temperature of the PV surface can still be observed, as depicted in Figs. 9 and 10. This could be attributed to the uneven heat distribution on the PV surface, especially in areas with no PCM.
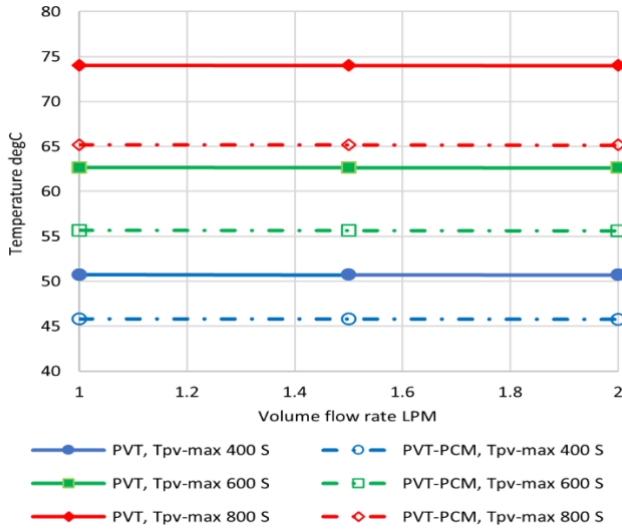
Fig. 9 Simulation finding for the changes in PV surface's maximum temperature with various mass flow rates
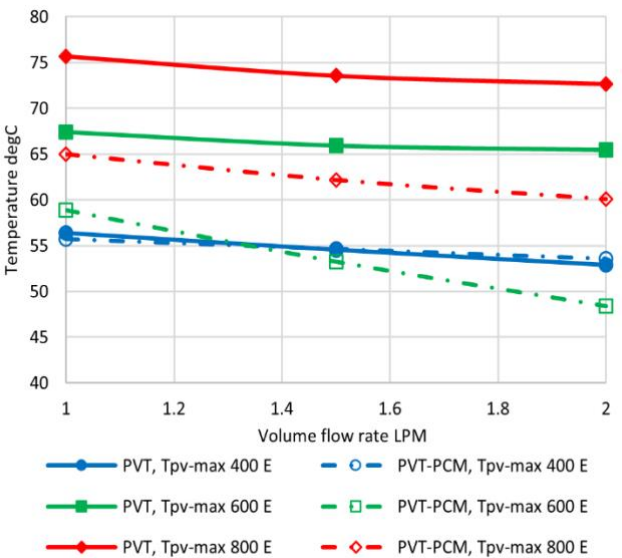
Fig.10 Experimental findings for the changes in PV surface's maximum temperature with various mass flow rates

3.2. . *Effect of mass flow rate on PV panel efficiency*

Since efficiency decreases with increasing temperature, the average surface temperature directly impacts the PV cell's efficiency. Figs. 11 and 12 illustrate the average surface temperature and electrical efficacy as a function of the experimental volume flow rate.

Fig. 13 shows the effect of solar radiation on the I-V and PV properties of the photovoltaic cell measured at PVT and PVT-PCM at irradiance of 800W/m². In Fig. 13, it can be observed that an increase in solar radiation leads to an increase in the current and voltage of the PV cell. However, the voltage decreases slightly at higher solar radiation levels while the current increases. As a result, the power output of the PV cell increases with increasing solar radiation up to a certain point, beyond which it starts to decrease due to the decrease in voltage. Additionally, as the volume flow rate increases, the PV cell's temperature decreases, leading to increased PV efficiency. Compares the thermal efficiency of the PVT, which is difficult to evaluate due to varying factors such as technology, absorber tube design, location, and configuration in previous studies.
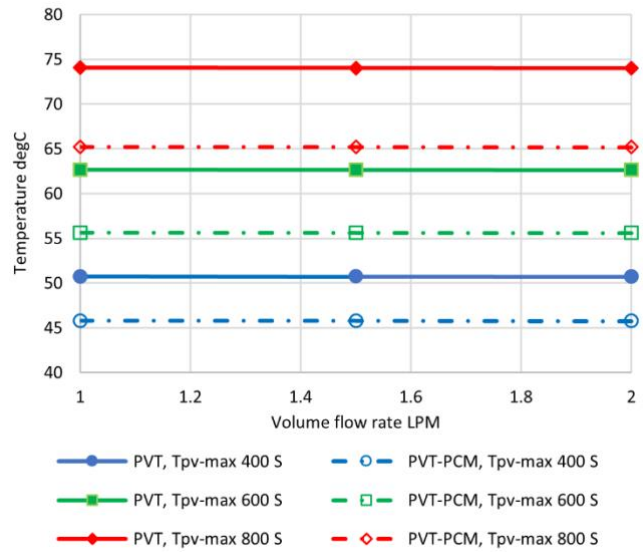
Fig. 11 Simulation finding for the changes in PV surface's maximum temperature with various mass flow rates
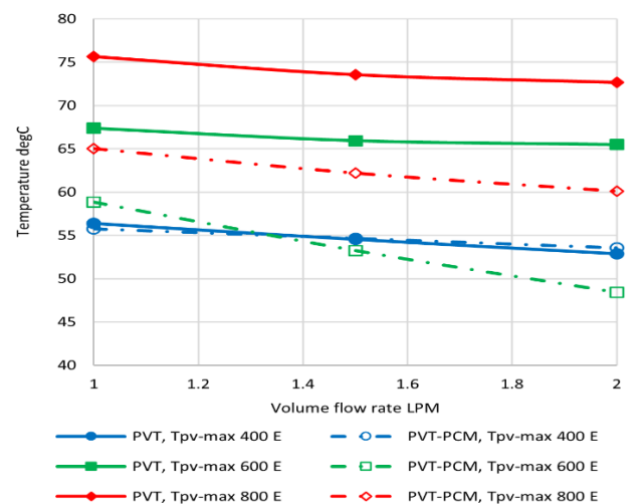
Fig. 12 Experimental findings for the changes in PV surface's maximum temperature with various mass flow rates
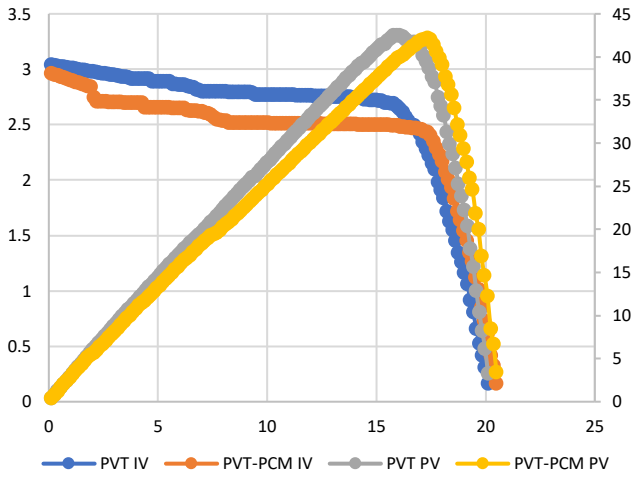
Fig. 13 I-V and P-V of PV Characteristics

Fig. 14 compares the thermal efficiency of the PVT, which is difficult to evaluate due to varying factors such as technology, absorber tube design, location, and configuration in previous studies.
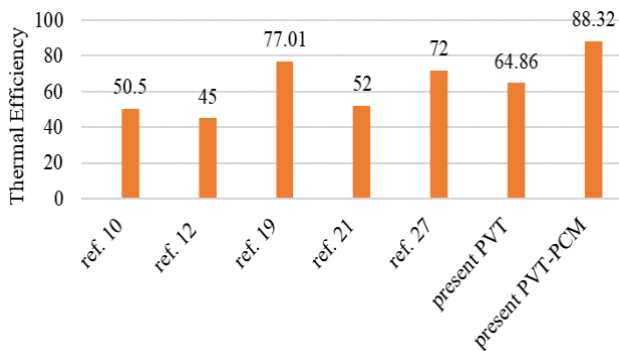
Fig.14 Comparisons of PVT and PVT-PCM in the literature and the present work

4. Conclusion

This research compares the electrical and thermal efficiencies of the PVT and PVT-PCM systems. The simulation was conducted under stable conditions, while the experiment was conducted in a laboratory. Comparing both systems, the performance indicated that the PCM system displays greater efficiency for all volume flow rate conditions. The higher the volume flow rate, the higher the cooling effect of the solar panel, and therefore, higher electrical efficiency is obtained. The greater the volume flow rate, the higher the thermal efficacy, even in case the difference of temperatures between the outflowing and incoming water is less. The study revealed that using square tubes in PVT-PCM configurations enhances thermal efficiency, and future research could explore the utilization of nanofluids to overcome the low thermal conductivity of water and further enhance system performance.

References

[1] W. E., Ewe, A. Fudholi, K. Sopian, and N. Asim, "Modeling of bifacial photovoltaic-thermal (PVT) air heater with jet plate," *Int. J. Heat Technol.*, vol. 39, no. 4, pp. 1117–1122, Aug. 2021, doi: 10.18280/ijht.390409.

[2] W. E., Ewe, A. Fudholi, K. Sopian, R. Moshery, N. Asim, W. Nuriana, and A. Ibrahim, "Thermo-electro-hydraulic analysis of jet impingement bifacial photovoltaic thermal (JIBPVT) solar air collector," *Energy*, vol. 254, p. 124366, 2022, doi: 10.1016/j.energy.2022.124366.

[3] W. E., Ewe, A. Fudholi, K. Sopian, N. Asim, Y. Ahmudiarto, and A. Salim, "Overview on Recent PVT Systems with Jet Impingement," *Int. J. Heat Technol.*, vol. 39, no. 6, pp. 1951–1956, 2021, doi: 10.18280/ijht.390633.

[4] M. A. M., Rosli, Y. J. Ping, S. Misha, M. Z. Akop, K. Sopian, S. Mat, A. N. Al-Shamani, and M. A. Saruni, "Simulation study of computational fluid dynamics on photovoltaic thermal water collector with different designs of absorber tube," *J. Adv. Res. Fluid Mech. Therm. Sci.*, vol. 52, no. 1, pp. 12–22, 2018.

[5] N., Katsumata, Y. Nakada, T. Minemoto, and H. Takakura, "Estimation of irradiance and outdoor performance of photovoltaic modules by meteorological data," *Sol. Energy Mater. Sol. Cells*, vol. 95, no. 1, pp. 199–202, 2011, doi: 10.1016/j.solmat.2010.01.019.

[6] E., Açıkkalp, H. Caliskan, H. Hong, H. Piao, and D. Seung, "Extended exergy analysis of a photovoltaic-thermal (PVT) module based desiccant air cooling system for buildings," *Appl. Energy*, vol. 323, no. February, p. 119581, 2022, doi: 10.1016/j.apenergy.2022.119581.

[7] M., Herrando, C. N. Markides, and K. Hellgardt, "A UK-based assessment of hybrid PV and solar-thermal systems for domestic heating and power: System performance," *Appl. Energy*, vol. 122, pp. 288–309, 2014, doi: 10.1016/j.apenergy.2014.01.061.

[8] N., Aste, F. Leonforte, and C. Del Pero, "Design, modeling and performance monitoring of a photovoltaic-thermal (PVT) water collector," *Sol. Energy*, vol. 112, pp. 85–99, 2015, doi: 10.1016/j.solener.2014.11.025.

[9] M. A. A. Bin., Ishak, "Performance of A Reversed Circular Flow Jet Impingement Bifacial PVT Solar

Collector," *Thesis, Univ. Kebangs. Malaysia*, 2023.

[10] M. A. A. B., Ishak, A. Ibrahim, K. Sopian, M. F. Fauzan, M. A. A. Rahmat, and N. J. Yusaidi, "Performance and Economic Analysis of a Reversed Circular Flow Jet Impingement Bifacial PVT Solar Collector," *Int. J. Renew. Energy Dev.*, vol. 12, no. 4, pp. 780–788, 2023, doi: https://doi.org/10.14710/ijred.2023.54348.

[11] V. Delisle, and M. Kummert, "Cost-benefit analysis of integrating BIPV-T air systems into energy-efficient homes," *Sol. Energy*, vol. 136, pp. 385–400, 2016, doi: 10.1016/j.solener.2016.07.005.

[12] A., Ibrahim, M. Y. Othman, M. H. Ruslan, S. Mat, and K. Sopian, "Recent advances in flat plate photovoltaic/thermal (PV/T) solar collectors," *Renew. Sustain. Energy Rev.*, vol. 15, no. 1, pp. 352–365, 2011, doi: 10.1016/j.rser.2010.09.024.

[13] M. B. A., Syazwan, A. Ibrahim, M. Amir, and A. Bin, "Energy performance evaluation of a photovoltaic thermal phase change material (PVT-PCM) using a spiral flow configuration," no. xx, 2022.

[14] M. A. A., Rahmat, A. S. A. Hamid, Y. Lu, M. A. A. B. Ishak, S. Z. Suheel, A. Fazlizan, and A. Ibrahim, "An Analysis of Renewable Energy Technology Integration Investments in Malaysia Using HOMER Pro," *Sustain.*, vol. 14, no. 20, 2022, doi: 10.3390/su142013684.

[15] M. A. A. B., Ishak, A. Ibrahim, A. Fazlizan, M. F. Fauzan, K. Sopian, and M. A. A. Rahmat, "Exergy performance of a reversed circular flow jet impingement bifacial photovoltaic thermal (PVT) solar collector," *Case Stud. Therm. Eng.*, vol. 49, 2023, doi: 10.1016/j.csite.2023.103322.

[16] A., Ibrahim, K. Sopian, M. Y. Othman, and A. Zaharim, "Simulation of different configuration of hybrid Photovoltaic Thermal Solar Collector (PVTS) Designs," 2008. [Online]. Available: https://api.semanticscholar.org/CorpusID:55995653

[17] M., Kingsley-amaehule, R. Uhunmwangho, N. Nwazor, and E. Kenneth, "Smart Intelligent Monitoring and Maintenance Management of Photo-voltaic Systems," *Int. J. Smart grid IJSMARTGRID*, vol. 6, no. 4, 2022, doi: https://doi.org/10.20508/ijsmartgrid.v6i4.260.g246.

[18] F., Javed, "Impact of Temperature & Illumination for Improvement in Photovoltaic System Efficiency," *Int. J. Smart grid IJSMARTGRID*, vol. 6, no. v6i1, 2022, doi: 10.20508/ijsmartgrid.v6i1.222.g185.

[19] A., Ibrahim, M. Y. Othman, M. H. Ruslan, M. A. Alghoul, M. Yahya, A. Zaharim, and K. Sopian, "Performance of photovoltaic thermal collector (PVT) with different absorbers design," *WSEAS Trans. Environ. Dev.*, vol. 5, no. 3, pp. 321–330, 2009.

[20] A., Ibrahim, G. L. Jin, R. Daghigh, M. H. M. Salleh, M. Y. Othman, M. H. Ruslan, S. Mat, and K. Sopian, "Hybrid Photovoltaic Thermal (PV/T) Air and Water Based Solar Collectors Suitable for Building Integrated Applications," *Am. J. Environ. Sci.*, vol. 5, no. 5, pp. 618–624, Oct. 2009, doi: 10.3844/ajessp.2009.618.624.

[21] J. C. Franklin, and M. Chandrasekar, "Performance enhancement of a single pass solar photovoltaic thermal system using staves in the trailing portion of the air channel," *Renew. Energy*, vol. 135, pp. 248–258, 2019, doi: 10.1016/j.renene.2018.12.004.

[22] M., Tirsu, N. Covalenco, D. Zaitsev, I. Negura, M. Gavrilas, and B. C. Neagu, "Photovoltaic-Thermal System for Trigenerating Electricity, Hot Water and Cold," in *2021 International Conference on Electromechanical and Energy Systems (SIELMEN)*, 2021, pp. 92–96. doi: 10.1109/SIELMEN53755.2021.9600378.

[23] M., Barbu, E. Minciuc, D. C. Frusescu, and D. Tutica, "Integration of Hybrid Photovoltaic Thermal Panels (PVT) in the District Heating System of Bucharest, Romania," in *2021 10th International Conference on ENERGY and ENVIRONMENT (CIEM)*, 2021, pp. 1–5. doi: 10.1109/CIEM52821.2021.9614721.

[24] S., Hassani, R. Saidur, S. Mekhilef, and R. A. Taylor, "Environmental and exergy benefit of nanofluid-based hybrid PV/T systems," *Energy Convers. Manag.*, vol. 123, pp. 431–444, 2016, doi: https://doi.org/10.1016/j.enconman.2016.06.061.

[25] K. Muthukarupan S., S. Eashwar S., V. Subramanian, S. Tiwari, and D. B. Singh, "Performance improvement of PVT module with applications of nano-fluids and phase change materials: A review," in *2020 International Conference on Electrical and Electronics Engineering (ICE3)*, 2020, pp. 767–772. doi: 10.1109/ICE348803.2020.9122832.

[26] A., Gaur, C. Ménézo, and S. Giroux--Julien, "Numerical studies on thermal and electrical performance of a fully wetted absorber PVT collector with PCM as a storage medium," *Renew. Energy*, vol. 109, pp. 168–187, 2017, doi: https://doi.org/10.1016/j.renene.2017.01.062.

[27] H., Fayaz, N. A. Rahim, M. Hasanuzzaman, R. Nasrin, and A. Rivai, "Numerical and experimental investigation of the effect of operating conditions on performance of PVT and PVT-PCM," *Renew. Energy*, vol. 143, pp. 827–841, 2019, doi: https://doi.org/10.1016/j.renene.2019.05.041.

[28] S. Kyaligonza, and E. Cetkin, "Photovoltaic System Efficiency Enhancement with Thermal Management: Phase Changing Materials (PCM) with High Conductivity Inserts," *Int. J. Smart grid*, vol. 5, no. 4, pp. 138–148, 2021, doi: 10.20508/ijsmartgrid.v5i4.218.g171.

[29] H. A., Kazem, A. H. A. Al-Waeli, M. T. Chaichan, K. H. Al-Waeli, A. B. Al-Aasam, and K. Sopian, "Evaluation and comparison of different flow

configurations PVT systems in Oman: A numerical and experimental investigation," *Sol. Energy*, vol. 208, no. February, pp. 58–88, 2020, doi: 10.1016/j.solener.2020.07.078.

[30] A. H. A., Al-Waeli, K. Sopian, H. A. Kazem, and M. T. Chaichan, "Evaluation of the electrical performance of a photovoltaic thermal system using nano-enhanced paraffin and nanofluids," *Case Stud. Therm. Eng.*, vol. 21, p. 100678, 2020, doi: https://doi.org/10.1016/j.csite.2020.100678.

[31] B. Sutanto, and Y. S. Indartono, "Computational fluid dynamic (CFD) modelling of floating photovoltaic cooling system with loop thermosiphon," *AIP Conf. Proc.*, vol. 2062, no. 1, p. 20011, 2019, doi: 10.1063/1.5086558.

[32] W., Fan, G. Kokogiannakis, and Z. Ma, "Optimisation of life cycle performance of a double-pass photovoltaic thermal-solar air heater with heat pipes," *Renew. Energy*, vol. 138, pp. 90–105, 2019, doi: 10.1016/j.renene.2019.01.078.

[33] R. K., Ajeel, W. S.-I. Salim, K. Sopian, M. Z. Yusoff, K. Hasnan, A. Ibrahim, and A. H. A. Al-Waeli, "Turbulent convective heat transfer of silica oxide nanofluid through corrugated channels: An experimental and numerical study," *Int. J. Heat Mass Transf.*, vol. 145, p. 118806, 2019, doi: https://doi.org/10.1016/j.ijheatmasstransfer.2019.118806.

[34] A., Ibrahim, A. Fudholi, K. Sopian, M. Y. Othman, and M. H. Ruslan, "Efficiencies and improvement potential of building integrated photovoltaic thermal (BIPVT) system," *Energy Convers. Manag.*, vol. 77, pp. 527–534, 2014, doi: https://doi.org/10.1016/j.enconman.2013.10.033.

[35] A. F., Ismail, A. S. A. Hamid, A. Ibrahim, H. Jarimi, and K. Sopian, "Performance Analysis of a Double Pass Solar Air Thermal Collector with Porous Media Using Lava Rock," *Energies*, vol. 15, no. 3, 2022, doi: 10.3390/en15030905.

[36] H., Kadri, "Comparison Between the Most Popular Structures of Multilevel Inverters and the Packed U Cell Structure," *Int. J. Smart grid IJSMARTGRID*, vol. 7, no. 3, 2023.

[37] S. Salim, and A. I. Tolago, "Use of Coconut Shell Become an Alternative Electricity," *Int. J. Smart grid IJSMARTGRID*, vol. 7, no. 3, 2023.

[38] K. O., Adu-Kankam, and L. Camarinha-matos, "Delegating Autonomy on Digital Twins in Energy Ecosystems," *Int. J. Smart grid IJSMARTGRID*, vol. 6, no. 4, 2022.

[39] A. H. A., Al-Waeli, M. T. Chaichan, K. Sopian, H. A. Kazem, H. B. Mahood, and A. A. Khadom, "Modeling and experimental validation of a PVT system using nanofluid coolant and nano-PCM," *Sol. Energy*, vol. 177, pp. 178–191, 2019, doi: https://doi.org/10.1016/j.solener.2018.11.016.

[40] S., Dubey, J. N. Sarvaiya, and B. Seshadri, "Temperature Dependent Photovoltaic (PV) Efficiency and Its Effect on PV Production in the World – A Review," *Energy Procedia*, vol. 33, pp. 311–321, 2013, doi: https://doi.org/10.1016/j.egypro.2013.05.072.

[41] K., Sopian, A. H. A. Al-Waeli, and H. A. Kazem, "Energy, exergy and efficiency of four photovoltaic thermal collectors with different energy storage material," *J. Energy Storage*, vol. 29, p. 101245, 2020, doi: https://doi.org/10.1016/j.est.2020.101245.